西南大學

天体核合成相关的原子核弱衰变过程

Longjun Wang

Southwest University, Chongqing, China

Jan. 11, 2026

含弘光大 继往开来 特立西南 学行天下

Outline

1. Introduction
2. Stellar weak rates
3. s process: branching point, thermometer
4. rp process: waiting points
5. Uncertainty in Gamow-Teller transition
6. Summary

Chart of nuclides

Nuclear Chart: decay mode of the ground state nuclide(NUBASE2020)

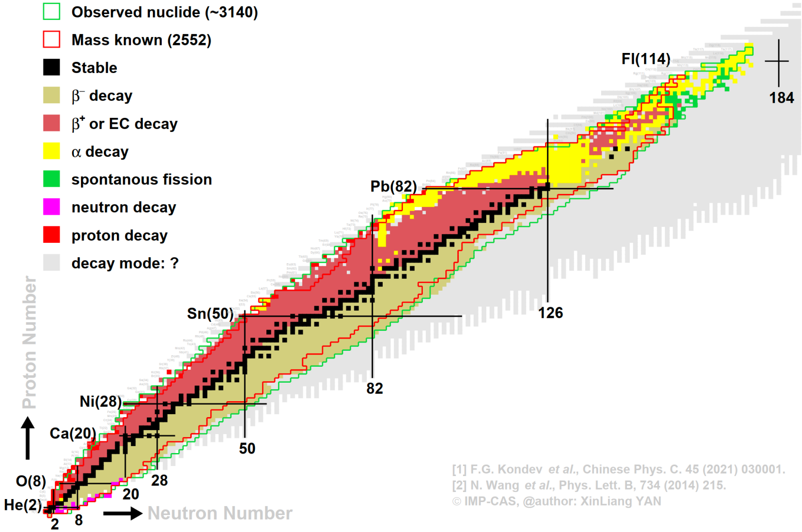

[1] F.G. Kondev *et al.*, Chinese Phys. C. 45 (2021) 030001.
[2] N. Wang *et al.*, Phys. Lett. B, 734 (2014) 215.
© IMP-CAS, @author: XinLiang YAN

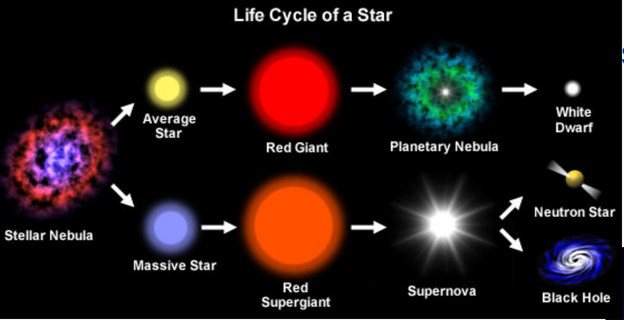

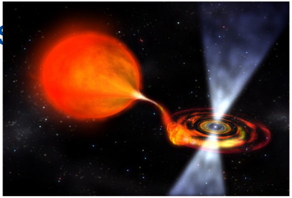

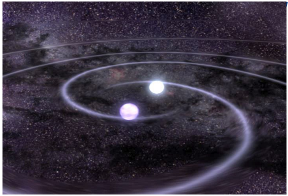

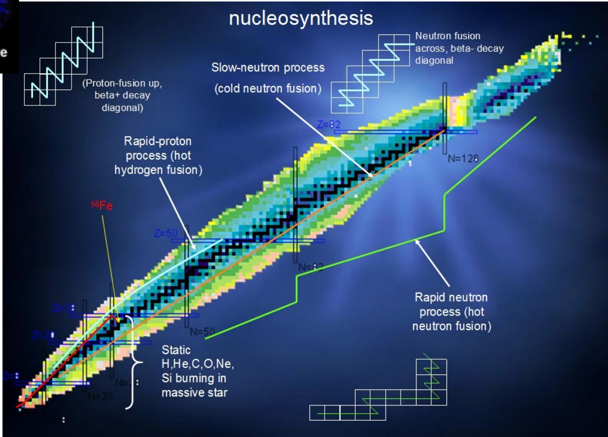

β decay: *high temperature and density, strong magnetic field.*

ν emission: *cooling mechanisms.*

neutron/proton capture: γ *strength function, level density.*

元素起源：核结构

西南大學

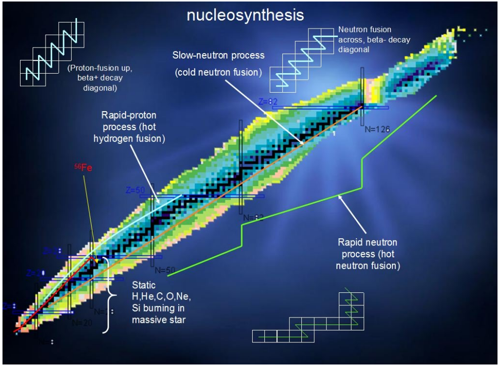

Neutron-capture rates

β decay rates

optical potential

Stellar weak rates

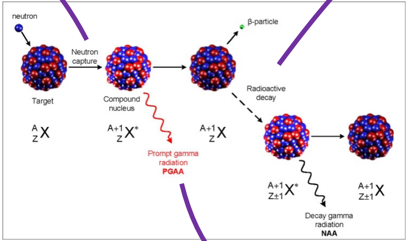

Nuclear level density

γ-ray strength function

$$\sigma_{n,\gamma}(E_n) \propto \sum \frac{T_n T_\gamma}{T_n + T_\gamma} \approx \sum T_\gamma$$

$$T_\gamma = \sum_{J^\pi, XL} \int_0^{S_n + E_n} 2\pi\, E_\gamma^{2L+1} f_{XL}(E_\gamma)\, \rho(E_x - E_\gamma, J, \pi)\, dE_\gamma$$

Wiedeking et al., Nature Rev. Phys. (2025)

s process: branching point

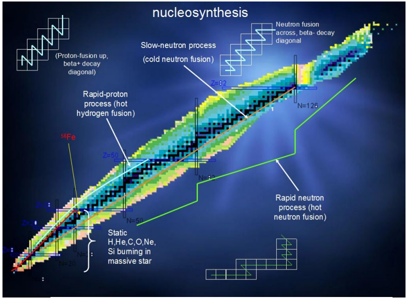

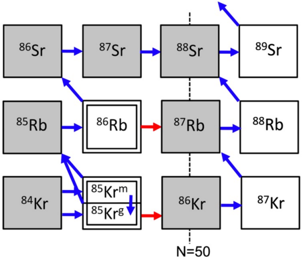

Raut et al., PRL 111, 112501 (2013)

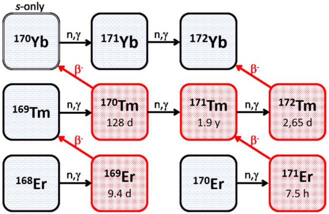

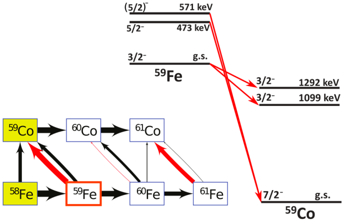

Guerrero et al., PRL 125, 142701 (2020)

Gao et al., PRL 126, 152701 (2021)

s process: thermometer

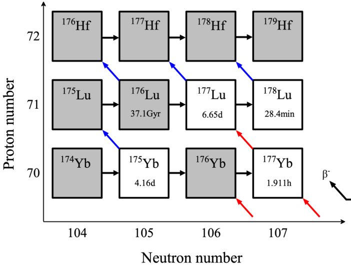

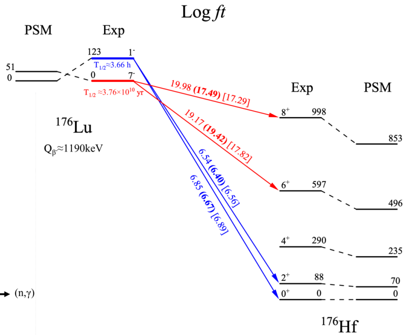

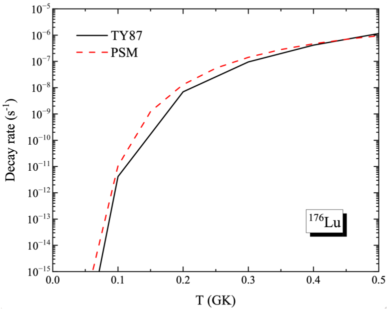

J.-W. Ran, LJW, Phys. Lett. B (2026)*

r process: core-collapse supernova

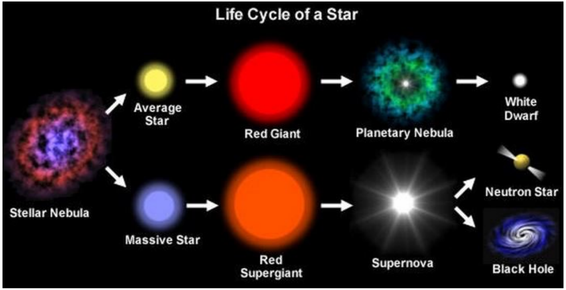

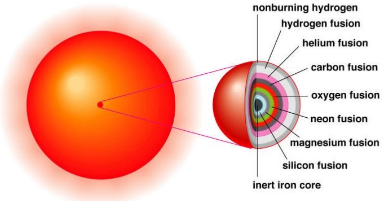

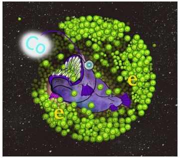

$$ {}^{A}_{Z}\mathrm{X} + e^- \to {}^{A}_{Z-1}\mathrm{Y} + \nu_e $$

- Reduce pressure from degenerate relativistic electron gas
- cooling environment by neutrinos
- drive the composition to be more neutron-rich

rp process: accreting neutron star

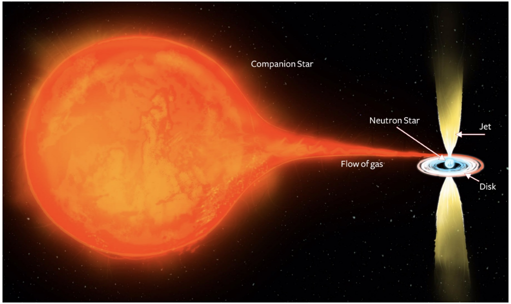

- ✓ X-ray bursts
- ✓ X-ray pulsars

- Urca cooling

$$\text{EC}: \quad {}^{A}_{Z}\text{X} + e^- \rightarrow {}^{A}_{Z-1}\text{Y} + \nu_e$$
$$\beta^-: \quad {}^{A}_{Z-1}\text{Y} \rightarrow {}^{A}_{Z}\text{X} + e^- + \bar{\nu}_e$$

H. Schatz et al., Nature (2014)

L.-J. Wang et al., Phys. Rev. Lett. (2021)

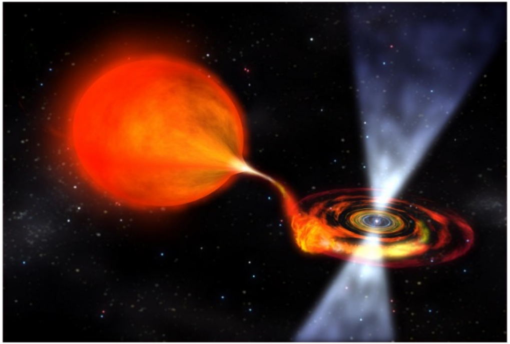

rp process: waiting-point nuclei

X-ray bursts:
H and He are fused eplosively up to Te within short time (10-100s)

Energy production through rp-process
Rapid proton captures vs. beta decay

Duration and the shape of the observed light curves

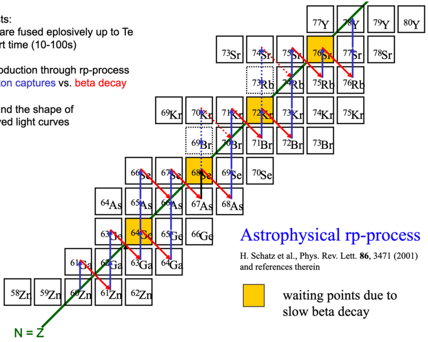

from Jokinen's slides

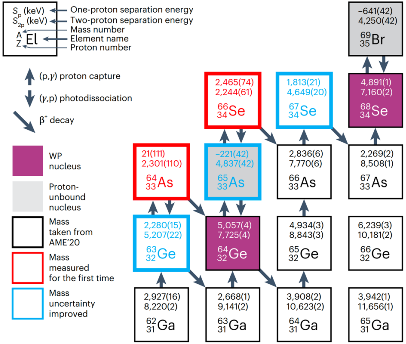

X. Zhou et al., Nat. Phys. (2023)

Stellar sites and conditions

- s process: *Rev. Mod. Phys 83, 157 (2011)*
  - AGB star and/or Core He & shell C of massive stars
  - $\rho Y_e \approx 10^{2-4}$ mol/cm^3? $T \approx 0.5$ GK? low magnetic field?
- rp process: *Phys Rep 294, 167 (1998); Science 355, 817 (2017)*
  - Accreting neutron stars (LMXBs and/or HMXBs)
  - $\rho Y_e \approx 10^{5-7}$ mol/cm^3? $T \approx 1.0$ GK, high magnetic field (10^{8-14} G)?
- r process: *Rev. Mod. Phys 93, 015002 (2021)*
  - Core-collapse supernovae and/or neutron-star merger and/or magnetar
  - $\rho Y_e \approx 10^{7-11}$ mol/cm^3? $T \approx 3.0$ GK, high magnetic field (10^{12-17} G)?

Stellar weak rates: many aspects

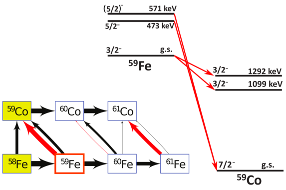

Gao et al., PRL 126, 152701 (2021)

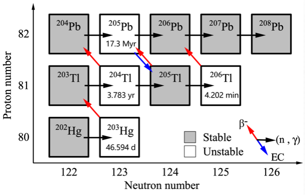

Xiao, LJW, PRC 110, 015806 (2024)

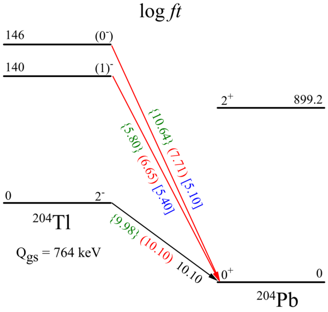

- Ground states, low- & high-lying states.
- Allowed & (1^{st}) forbidden transitions.

$$\lambda^{\beta^-} = \sum_{if} \frac{(2J_i+1)e^{-E_i/k_BT}}{G(Z,A,T)} \lambda_{if}^{\beta^-}, \quad (1)$$

$$\lambda_{if}^{\beta^-} = \frac{\ln 2}{K} \int_1^{Q_{if}} C(W)F(Z,W)pW(Q_{if}-W)^2[1-S_e(W)]dW. \quad (2)$$

- High density and temperature, Strong magnetic field.
- Systematical calculation from light to heavy nuclei.

Outline

1. Introduction

2. Stellar weak rates

3. s process: branching point, thermometer

4. rp process: waiting points

5. Uncertainty in Gamow-Teller transition

6. Summary

Stellar weak rates

$$\beta^- : {}^A_Z\mathrm{X} \to {}^{\;\;A}_{Z+1}\mathrm{Y} + e^- + \bar{\nu}_e, \qquad \mathrm{EC} : {}^A_Z\mathrm{X} + e^- \to {}^{\;\;A}_{Z-1}\mathrm{Y} + \nu_e,$$
$$\beta^+ : {}^A_Z\mathrm{X} \to {}^{\;\;A}_{Z-1}\mathrm{Y} + e^+ + \nu_e, \qquad \mathrm{PC} : {}^A_Z\mathrm{X} + e^+ \to {}^{\;\;A}_{Z+1}\mathrm{Y} + \bar{\nu}_e,$$

- Without magnetic field:

$$\lambda^\alpha = \sum_{if} \frac{(2J_i+1)e^{-E_i/k_BT}}{G(Z,A,T)} \lambda^\alpha_{if}$$

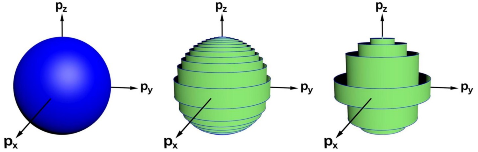

$$\lambda^{\beta^-}_{if} = \frac{\ln 2}{K}\int_1^{Q_{if}} \boldsymbol{C(W)} F_0(Z+1,W)pW(Q_{if}-W)^2[1-S_e(W)]dW, \quad (3)$$

$$\lambda^{\mathrm{EC}}_{if} = \frac{\ln 2}{K}\int_{\omega_l}^{\infty} \boldsymbol{C(W)} F_0(Z,W)pW(Q_{if}+W)^2 S_e(W)dW, \quad (4)$$

$$\lambda^{\beta^+}_{if} = \frac{\ln 2}{K}\int_1^{Q_{if}} \boldsymbol{C(W)} F_0(-Z+1,W)pW(Q_{if}-W)^2[1-S_p(W)]dW, \quad (5)$$

$$\lambda^{\mathrm{PC}}_{if} = \frac{\ln 2}{K}\int_{\omega_l}^{\infty} \boldsymbol{C(W)} F_0(-Z,W)pW(Q_{if}+W)^2 S_p(W)dW, \quad (6)$$

$$\rho Y_e = \frac{1}{\pi^2 N_A}\left(\frac{m_e c}{\hbar}\right)^3 \int_0^\infty (S_e - S_p)p^2 dp, \qquad S_{e/p}(\omega) = \frac{1}{\exp[(\omega \mp \mu_e)/k_B T)] + 1}, \quad (7)$$

Stellar weak rates

$$\beta^- : {}^A_Z\text{X} \to {}^{\;\;A}_{Z+1}\text{Y} + e^- + \bar{\nu}_e, \qquad \text{EC} : {}^A_Z\text{X} + e^- \to {}^{\;\;A}_{Z-1}\text{Y} + \nu_e,$$

$$\beta^+ : {}^A_Z\text{X} \to {}^{\;\;A}_{Z-1}\text{Y} + e^+ + \nu_e, \qquad \text{PC} : {}^A_Z\text{X} + e^+ \to {}^{\;\;A}_{Z+1}\text{Y} + \bar{\nu}_e,$$

- With strong magnetic field: *Hu, LJW*, Sun: PRL (2025)*

$$\lambda^\alpha = \sum_{if} \frac{(2J_i+1)e^{-E_i/k_BT}}{G(Z,A,T)} \lambda^\alpha_{if}$$

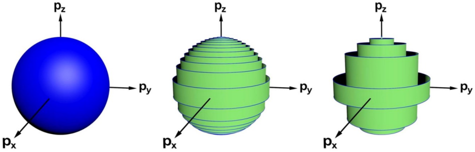

$$\lambda^{\beta^-}_{if} = \frac{\ln 2}{K}\frac{B^*}{2}\sum_{n=0}^{N_{\rm max}}(2-\delta_{n0})\int_0^{\sqrt{Q_{if}^2-1-2nB^*}} \boldsymbol{C(W)} F_0(Z+1,W)(Q_{if}-W)^2[1-S_e(W)]dp_z, \qquad (8)$$

$$\lambda^{\rm EC}_{if} = \frac{\ln 2}{K}\frac{B^*}{2}\sum_{n=0}^{N_{\rm max}}(2-\delta_{n0})\int_{p_{znl}}^{\infty} \boldsymbol{C(W)} F_0(Z,W)(Q_{if}+W)^2 S_e(W)dp_z, \qquad (9)$$

$$\lambda^{\beta^+}_{if} = \frac{\ln 2}{K}\frac{B^*}{2}\sum_{n=0}^{N_{\rm max}}(2-\delta_{n0})\int_0^{\sqrt{Q_{if}^2-1-2nB^*}} \boldsymbol{C(W)} F_0(-Z+1,W)(Q_{if}-W)^2[1-S_p(W)]dp_z, \qquad (10)$$

$$\lambda^{\rm PC}_{if} = \frac{\ln 2}{K}\frac{B^*}{2}\sum_{n=0}^{N_{\rm max}}(2-\delta_{n0})\int_{p_{znl}}^{\infty} \boldsymbol{C(W)} F_0(-Z,W)(Q_{if}+W)^2 S_p(W)dp_z, \qquad (11)$$

$$\rho Y_e = \frac{B^*}{2\pi^2 N_A \lambda_e^3}\sum_{n=0}^{N_{\rm lim}}(2-\delta_{n0})\int_0^\infty (S_e - S_p)dp_z, \qquad (12)$$

Stellar weak rates

$$\beta^- : {}^A_Z\mathrm{X} \to {}^{\ \ A}_{Z+1}\mathrm{Y} + e^- + \bar{\nu}_e, \qquad \mathrm{EC} : {}^A_Z\mathrm{X} + e^- \to {}^{\ \ A}_{Z-1}\mathrm{Y} + \nu_e,$$

$$\beta^+ : {}^A_Z\mathrm{X} \to {}^{\ \ A}_{Z-1}\mathrm{Y} + e^+ + \nu_e, \qquad \mathrm{PC} : {}^A_Z\mathrm{X} + e^+ \to {}^{\ \ A}_{Z+1}\mathrm{Y} + \bar{\nu}_e,$$

- With strong magnetic field: *Hu, LJW*, Sun: PRL (2025)*

$$\xi^\alpha = \sum_{if} \frac{(2J_i+1)e^{-E_i/k_BT}}{G(Z,A,T)} \xi^\alpha_{if}$$

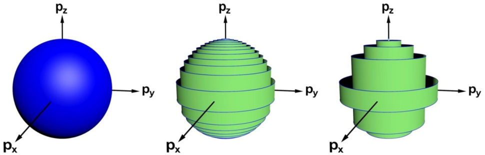

$$\xi^{\beta^-}_{if} = \frac{\ln 2}{K}\frac{B^* m_e c^2}{2}\sum_{n=0}^{N_{\max}}(2-\delta_{n0})\int_0^{\sqrt{Q_{if}^2-1-2nB^*}} \boldsymbol{C(W)} F_0(Z+1,W)(Q_{if}-W)^3[1-S_e(W)]dp_z, \quad (13)$$

$$\xi^{\mathrm{EC}}_{if} = \frac{\ln 2}{K}\frac{B^* m_e c^2}{2}\sum_{n=0}^{N_{\max}}(2-\delta_{n0})\int_{p_{znl}}^{\infty} \boldsymbol{C(W)} F_0(Z,W)(Q_{if}+W)^3 S_e(W)dp_z, \quad (14)$$

$$\xi^{\beta^+}_{if} = \frac{\ln 2}{K}\frac{B^* m_e c^2}{2}\sum_{n=0}^{N_{\max}}(2-\delta_{n0})\int_0^{\sqrt{Q_{if}^2-1-2nB^*}} \boldsymbol{C(W)} F_0(-Z+1,W)(Q_{if}-W)^3[1-S_p(W)]dp_z, \quad (15)$$

$$\xi^{\mathrm{PC}}_{if} = \frac{\ln 2}{K}\frac{B^* m_e c^2}{2}\sum_{n=0}^{N_{\max}}(2-\delta_{n0})\int_{p_{znl}}^{\infty} \boldsymbol{C(W)} F_0(-Z,W)(Q_{if}+W)^3 S_p(W)dp_z, \quad (16)$$

$$\rho Y_e = \frac{B^*}{2\pi^2 N_A \lambda_e^3}\sum_{n=0}^{N_{\lim}}(2-\delta_{n0})\int_0^{\infty}(S_e - S_p)dp_z, \quad (12)$$

Allowed transition: quenching puzzle

西南大學

- For allowed GT transition with $|\Delta J| = 0, 1;\ \Delta\pi = +$:

$$C(W) = B(\mathrm{GT}^{\pm})_{if} = \left(\frac{g_A}{g_V}\right)^2_{\text{eff}} \frac{\langle \Psi^{n_f}_{J_f} \| \sum_k \hat{\sigma}^k \hat{\tau}^k_{\pm} \| \Psi^{n_i}_{J_i} \rangle^2}{2J_i + 1} \tag{18}$$

- Transition operator quenching:

$$\left(\frac{g_A}{g_V}\right)_{\text{eff}} = f_{\text{quench}} \left(\frac{g_A}{g_V}\right)_{\text{bare}} \tag{19}$$

where $(g_A/g_V)_{\text{bare}} = -1.27641(45)$. $f_{\text{quench}} \approx 0.75$.

Martínez-Pinedo et al: PRC (1996R);
Brown, Wildenthal: ADNDT (1985);
Gao, Sun, Chen: PRC 74, 054303 (2006);
L.-J. Wang, Sun, Ghorui: PRC 97, 044302 (2018)
Tan, Liu, L.-J. Wang: PLB 805, 135432 (2020)*
Chen and L.-J. Wang: PLB 848, 138338 (2024)*
L.-J. Wang, Tan, Li, Misch, Sun: PRL 127, 172702 (2021);

First-forbidden transition

For first-forbidden non-unique ($|\Delta J|^\pi = 0^-, 1^-$) and unique ($|\Delta J|^\pi = 2^-$):

$$C(W) = (k + kaW + kb/W + kcW^2)[q^2 + \lambda_2 p^2]$$
$$k = [\zeta_0^2 + \frac{1}{9}w^2]^{(0)} + [\zeta_1^2 + \frac{1}{9}(x+u)^2 - \frac{4}{9}\mu_1\gamma_1 u(x+u)$$
$$+ \frac{1}{18}W_0^2(2x+u)^2 - \frac{1}{18}\lambda_2(2x-u)^2]^{(1)}$$
$$+ [\frac{1}{12}z^2(W_0^2 - \lambda_2)]^{(2)},$$
$$ka = [-\frac{4}{3}uY - \frac{1}{9}W_0(4x^2 + 5u^2)]^{(1)} - [\frac{1}{6}z^2 W_0]^{(2)},$$
$$kb = \frac{2}{3}\mu_1\gamma_1\{-[\zeta_0 w]^{(0)} + [\zeta_1(x+u)]^{(1)}\},$$
$$kc = \frac{1}{18}[8u^2 + (2x+u)^2 + \lambda_2(2x-u)^2]^{(1)}$$
$$+ \frac{1}{12}[z^2(1+\lambda_2)]^{(2)}$$
$$V = \xi'\nu + \xi w', \quad \zeta_0 = V + \frac{1}{3}wW_0,$$
$$Y = \xi' y - \xi(u' + x'), \quad \zeta_1 = Y + \frac{1}{3}(u-x)W_0.$$

$$w = -g_A\sqrt{3}\frac{\langle f\| \sum_k r_k [C_1^k \otimes \sigma^k]^0 \tau_-^k \|i\rangle}{\sqrt{2J_i+1}}$$
$$x = -\frac{\langle f\| \sum_k r_k C_1^k \tau_-^k \|i\rangle}{\sqrt{2J_i+1}}$$
$$u = -g_A\sqrt{2}\frac{\langle f\| \sum_k r_k [C_1^k \otimes \sigma^k]^1 \tau_-^k \|i\rangle}{\sqrt{2J_i+1}}$$
$$z = 2g_A\frac{\langle f\| \sum_k r_k [C_1^k \otimes \sigma^k]^2 \tau_-^k \|i\rangle}{\sqrt{2J_i+1}}$$
$$w' = -g_A\sqrt{3}\frac{\langle f\| \sum_k \frac{2}{3} r_k I(r_k) [C_1^k \otimes \sigma^k]^0 \tau_-^k \|i\rangle}{\sqrt{2J_i+1}}$$
$$x' = -\frac{\langle f\| \sum_k \frac{2}{3} r_k I(r_k) C_1^k \tau_-^k \|i\rangle}{\sqrt{2J_i+1}}$$
$$u' = -g_A\sqrt{2}\frac{\langle f\| \sum_k \frac{2}{3} r_k I(r_k) [C_1^k \otimes \sigma^k]^1 \tau_-^k \|i\rangle}{\sqrt{2J_i+1}}$$
$$\xi'\nu = \frac{g_A\sqrt{3}}{M}\frac{\langle f\| \sum_k [\sigma_k \otimes \nabla^k]^0 \tau_-^k \|i\rangle}{\sqrt{2J_i+1}}$$
$$\xi' y = -\frac{1}{M}\frac{\langle f\| \sum_k \nabla^k \tau_-^k \|i\rangle}{\sqrt{2J_i+1}}$$

H. Behrens, W. Bühring, NPA 162, 111 (1971);

Suzuki, Yoshida, Kajino, Otsuka, PRC 85, 015802 (2012);

Q. Zhi, E. Caurier et al., PRC 87, 025803 (2013);

Gao, Chen and L.-J. Wang: PRC (2023);*

B.-L. Wang and L.-J. Wang: PLB (2024);*

First-forbidden transition: quenching puzzle

- Shell-model quenching factors:

$$f_q(\xi'\nu) = 1.266, \qquad f_q(w) = f_q(w') = 0.66,$$
$$f_q(x) = f_q(x') = 0.51, \quad f_q(u) = f_q(u') = 0.38,$$
$$f_q(z) = 0.42.$$

Zhi, Caurier, Cuenca-García, Langanke, Martínez-Pinedo, Sieja: PRC 87, 025803 (2013)

B.-L. Wang, LJW, PLB (2024)*

Outline

1. Introduction
2. Stellar weak rates
3. s process: branching point, thermometer
4. rp process: waiting points
5. Uncertainty in Gamow-Teller transition
6. Summary

s-process: branching-point and thermometer ^{176}Lu

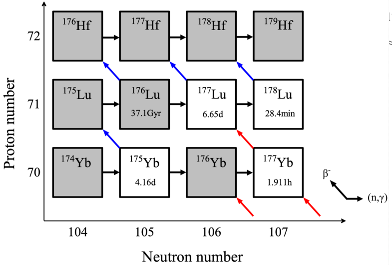

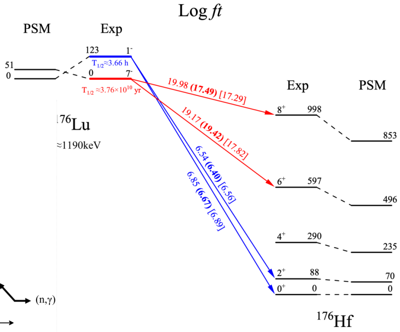

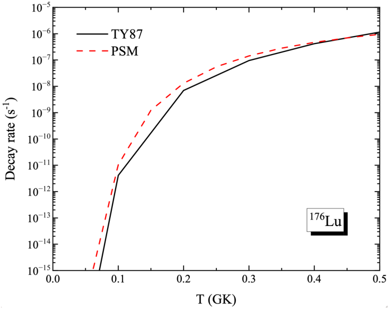

E. Scherer et al., Science (2001)
Y. Amelin et al., Science (2005)

J.-W. Ran, LJW, Phys. Lett. B (2026)*

s-process: branching-point and thermometer ^{176}Lu

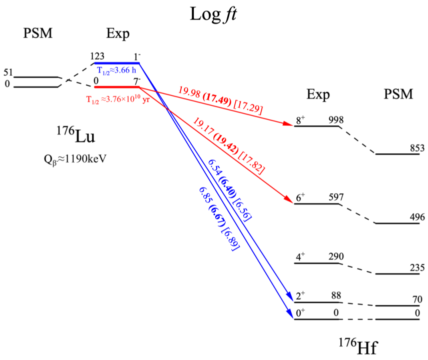

- ➢ **Anomalous strength:**
  the only two strange first-forbidden transitions with Log ft ≫ 12 in the known evaluated nuclear databases

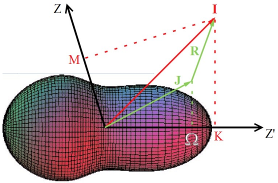

The $\log ft$ value, the configuration mixing percentage, and the average K value $\bar{K}$, from the PSM calculations with different configuration spaces (no mixing case, small configuration space and large configuration space, respectively) for the $7^- \to 6^+$ (8^+) first-forbidden transition of ^{176}Lu. See the text for details.

Transition	$7^- \longrightarrow 6^+$ (8^+)		
	No mixing	Small	Large
$\log ft$	19.95 (21.69)	17.82 (17.29)	19.42 (17.49)
Configuration mixing	0 0 (0)	3.96% 55.11% (64.00%)	39.16% 66.36% (72.96%)
$\bar{K}$	7 0 (0)	6.824 0.197 (0.320)	6.809 0.252 (0.276)

J.-W. Ran, LJW, Phys. Lett. B (2026)*

Outline

1. Introduction
2. Stellar weak rates
3. s process: branching point, thermometer
4. rp process: waiting points
5. Uncertainty in Gamow-Teller transition
6. Summary

rp process: waiting points

X-ray bursts:
H and He are fused eplosively up to Te
within short time (10-100s)

Energy production through rp-process
Rapid proton captures vs. beta decay

Duration and the shape of
the observed light curves

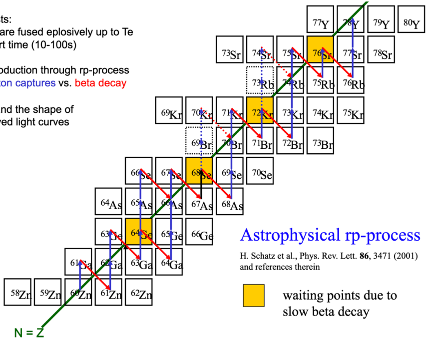

from Jokinen's slides

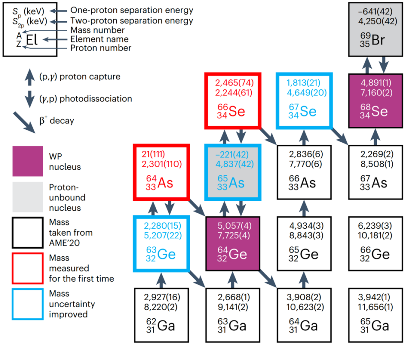

X. Zhou et al., Nat. Phys. (2023)

Waiting points: B(GT) distribution

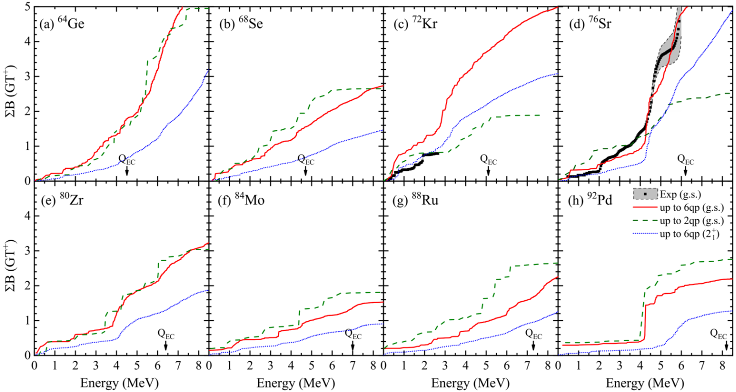

Chen, LJW, PLB (2024)*

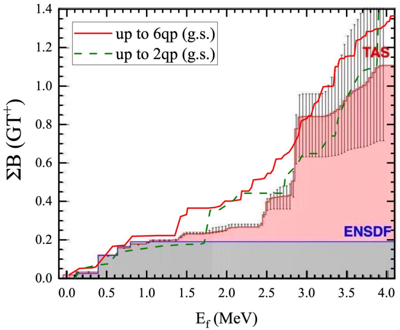

Enrique Nácher González,
Instituto de Física Corpuscular, CSIC - UV
(Private Communication)

Waiting points: weak rates

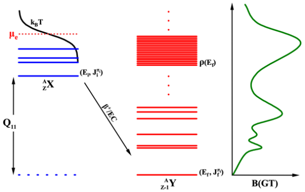

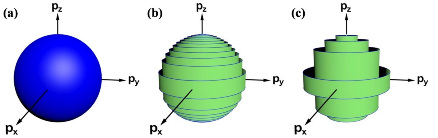

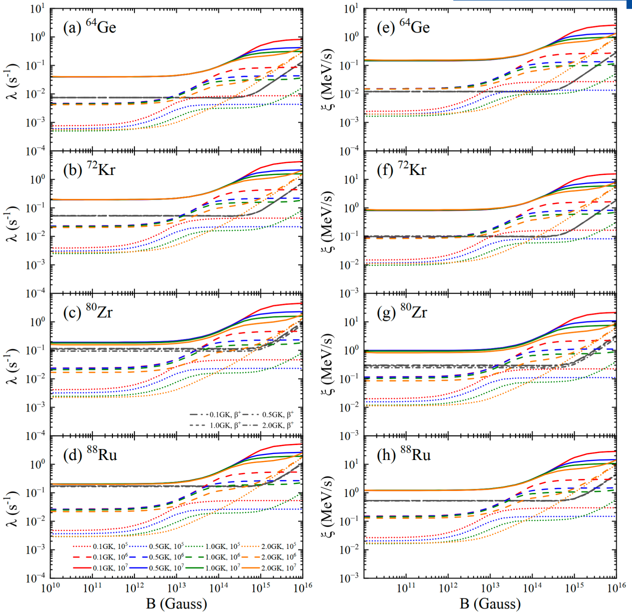

Hu, LJW, Sun, PRL 135, 042702 (2025)*

Outline

1. Introduction
2. Stellar weak rates
3. s process: branching point, thermometer
4. rp process: waiting points
5. Uncertainty in Gamow-Teller transition
6. Summary

g_A quenching puzzle

$$\lambda_{if}^{\beta^-} = \frac{\ln 2}{K}\int_1^{Q_{if}} \boldsymbol{C(W)} F_0(Z+1,W)pW(Q_{if}-W)^2[1-S_e(W)]dW,$$
$$\lambda_{if}^{\mathrm{EC}} = \frac{\ln 2}{K}\int_{\omega_l}^{\infty} \boldsymbol{C(W)} F_0(Z,W)pW(Q_{if}+W)^2 S_e(W)dW,$$

- For allowed GT transition with $|\Delta J| = 0, 1$; $\Delta\pi = +$:

$$C(W) = B(\mathrm{GT}^{\pm})_{if} = \left(\frac{g_A}{g_V}\right)^2_{\mathrm{eff}} \frac{\langle \Psi^{n_f}_{J_f} \| \sum_k \hat{\sigma}^k \hat{\tau}^k_{\pm} \| \Psi^{n_i}_{J_i}\rangle^2}{2J_i+1}$$

- Transition operator quenching:

$$\left(\frac{g_A}{g_V}\right)_{\mathrm{eff}} = f_{\mathrm{quench}}\left(\frac{g_A}{g_V}\right)_{\mathrm{bare}}$$

where $(g_A/g_V)_{\mathrm{bare}} = -1.27641(45)$. $f_{\mathrm{quench}} \approx 0.75$.

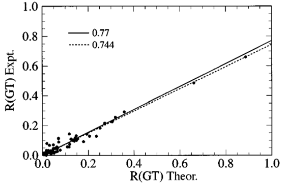

FIG. 1. Comparison of the experimental matrix elements $R(\mathrm{GT})$ with the theoretical calculations based on the "free-nucleon" Gamow-Teller operator. Each transition is indicated by a point in the x-y plane, with the theoretical value given by the x coordinate of the point and the experimental value by the y coordinate.

Martinez-Pinedo et al., PRC (1996)

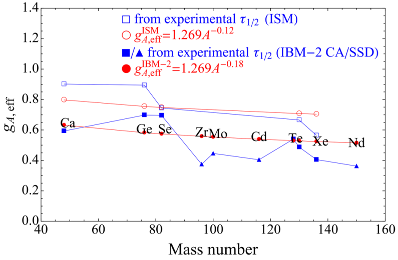

Chiral two-body current

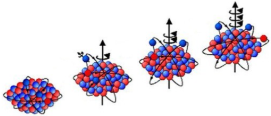

- β-decay transition matrix element:

$$\langle F|\hat{H}_\beta|I\rangle = -\frac{G_\beta}{\sqrt{2}} l^\mu \int d^3x \left\langle \Psi_{J_f M_f} \middle| e^{-i\boldsymbol{q}\cdot\boldsymbol{r}} J_\mu(\boldsymbol{x}) \middle| \Psi_{J_i M_i} \right\rangle , \tag{38}$$

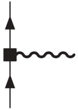

one-body $\hat{\boldsymbol{\sigma}}\hat{\tau}_\pm$

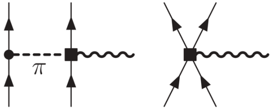

two-body

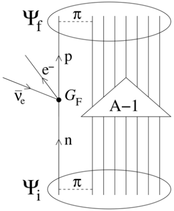

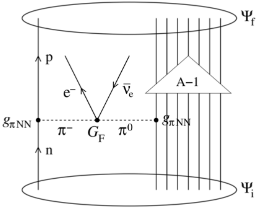

Menéndez, Gazit, Schwenk: PRL (2011);
L.-J. Wang, Engel, Yao: PRC (2018R);
Gysbers, Hagen, Holt et al., Nature Phys. (2019)
Ney, Engel, Schunck: PRC (2022)

H. Zhou, L.-J. Wang, Y. Sun: arXiv:2509.24542*

g_A quenching puzzle: two-body currents ?

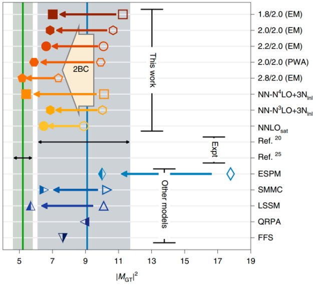

Fig. 1 | Gamow–Teller strength in ^{100}Sn. Comparison of the Gamow–Teller

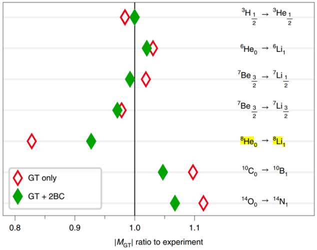

Fig. 2 | Gamow–Teller strengths in light nuclei. Theory-to-experiment ratio for the Gamow–Teller matrix elements of six strong transitions in light nuclei for the NN-N^{4}LO + 3N$_{lnl}$ interaction developed in this work.

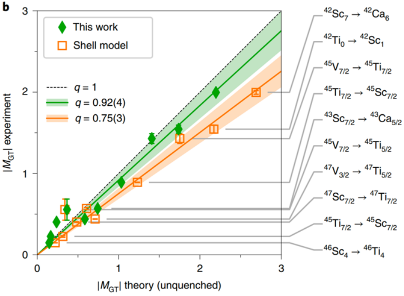

Fig. 3 | Gamow–Teller strengths in medium-mass nuclei. Comparison

Gysbers, Hagen, Holt et al., Nature Phys. (2019)

One-body and two-body currents

$$\hat{\mathcal{J}}_{1b}(\boldsymbol{x}) = -g_A \sum_{i=1}^{A} \boldsymbol{\sigma}_i \tau_i^- \delta(\boldsymbol{x}-\boldsymbol{r}_i), \tag{39}$$

$$\hat{\mathcal{J}}_{\rm 2b}(\boldsymbol{x}) \ = \sum_{k<l}^{A} \boldsymbol{J}_{kl}(\boldsymbol{x}), \tag{40}$$

$$\begin{aligned}\boldsymbol{J}_{kl}(\boldsymbol{x}) = & \frac{2c_3 g_A(q^2)}{m_N F_\pi^2}\left[m_\pi^2\left(\left(\frac{\boldsymbol{\sigma}_l}{3}-\boldsymbol{\sigma}_l \cdot \hat{\boldsymbol{r}}\hat{\boldsymbol{r}}\right)Y_2(r)-\frac{\boldsymbol{\sigma}_l}{3}Y_0(r)\right)+\frac{\boldsymbol{\sigma}_l}{3}\delta(\boldsymbol{r})\right]\boldsymbol{\tau}_l^-\delta(\boldsymbol{x}-\boldsymbol{r}_k) \ + \ (k\leftrightarrow l) \\ & + \left(c_4+\frac{1}{4}\right)\frac{g_A(q^2)}{2m_N F_\pi^2}\left[m_\pi^2\left(\left(\frac{\boldsymbol{\sigma}_\times}{3}-\boldsymbol{\sigma}_k\times\hat{\boldsymbol{r}}\boldsymbol{\sigma}_l \cdot \hat{\boldsymbol{r}}\right)Y_2(r)-\frac{\boldsymbol{\sigma}_\times}{3}Y_0(r)\right)+\frac{\boldsymbol{\sigma}_\times}{3}\delta(\boldsymbol{r})\right]\boldsymbol{\tau}_\times^-\delta(\boldsymbol{x}-\boldsymbol{r}_k) \ + \ (k\leftrightarrow l) \\ & - \frac{g_A(q^2)}{4m_N F_\pi^2}\left[2\hat{d}_1(\boldsymbol{\sigma}_k\boldsymbol{\tau}_k^- + \boldsymbol{\sigma}_l\boldsymbol{\tau}_l^-)+\hat{d}_2\boldsymbol{\sigma}_\times\boldsymbol{\tau}_\times^-\right]\delta(\boldsymbol{r})\delta(\boldsymbol{x}-\boldsymbol{r}_k).\end{aligned} \tag{41}$$

LJW, Engel, Yao, PRC 98, 031301(R) (2018)

For deformed nuclei

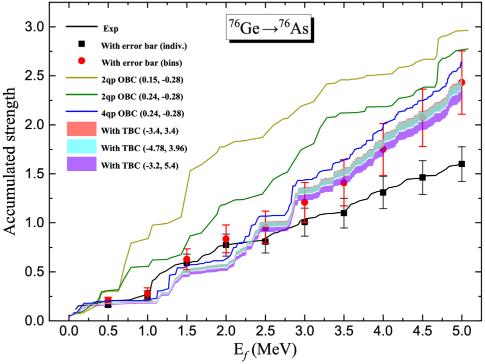

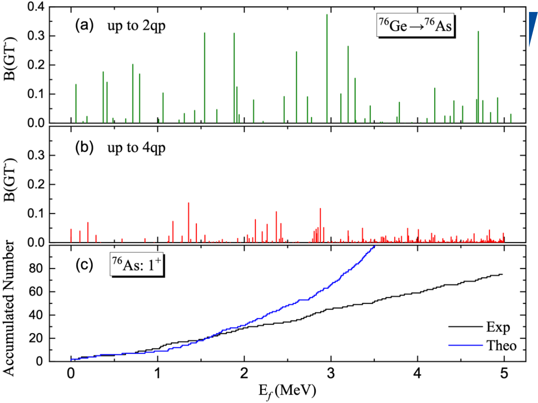

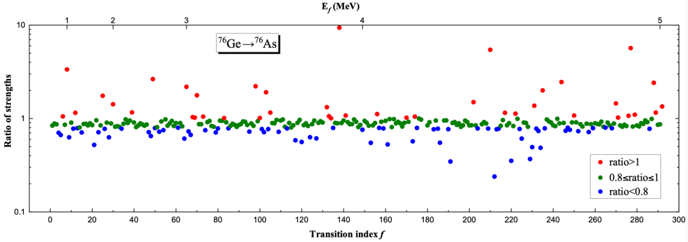

Zhou, LJW, Sun, arXiv: 2509. 24542*

High-lying region

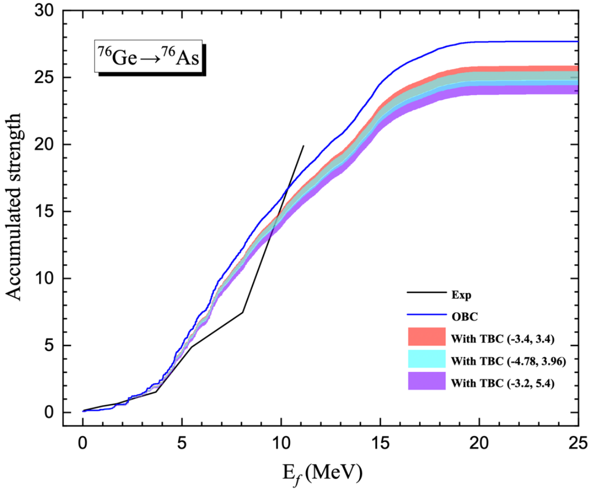

Zhou, LJW, Sun, arXiv: 2509. 24542*

Outline

1. Introduction
2. Stellar weak rates
3. s process: branching point, thermometer
4. rp process: waiting points
5. Uncertainty in Gamow-Teller transition
6. Summary

Summary and Outlook

- Basic ideas and pictures of the stellar weak rates.
- Effect of strong magnetic field on stellar weak rates of the *rp*-process waiting-point nuclei.
- Effect of chiral two-body currents on GT transition.

- Nuclear γ-ray strength function.
- Chiral two-body currents for $\beta\beta$ decay and γ transition.

Thank you and Welcome to Chongqing!